

REPORT DOCUMENTATION PAGE

Form Approved
OMB NO. 0704-0188

Public Reporting burden for this collection of information is estimated to average 1 hour per response, including the time for reviewing instructions, searching existing data sources, gathering and maintaining the data needed, and completing and reviewing the collection of information. Send comment regarding this burden estimates or any other aspect of this collection of information, including suggestions for reducing this burden, to Washington Headquarters Services, Directorate for information Operations and Reports, 1215 Jefferson Davis Highway, Suite 1204, Arlington, VA 22202-4302, and to the Office of Management and Budget, Paperwork Reduction Project (0704-0188), Washington, DC 20503.

1. AGENCY USE ONLY (Leave Blank)		2. REPORT DATE February, 2006		3. REPORT TYPE AND DATES COVERED Final Technical Report	
4. TITLE AND SUBTITLE Development of K-Version of the Finite Element Method: A Robust Mathematical and Computational Procedure				5. FUNDING NUMBERS AFOSR Grant No. F49620-03-1-0201	
6. AUTHOR(S) J. N. Reddy					
7. PERFORMING ORGANIZATION NAME(S) AND ADDRESS(ES) Department of Mechanical Engineering, Texas A&M University College Station, Texas 77843-3123				8. PERFORMING ORGANIZATION REPORT NUMBER	
9. SPONSORING / MONITORING AGENCY NAME(S) AND ADDRESS(ES) Department of the Air Force Air Force Office of Scientific Research Directorate of Mathematics & Space Sciences Computational Mathematics Program 875 North Randolph Street, Suite 325, Room 3112 Arlington, VA 22203 AFRL-SR-AR-TR-06-0293					
11. SUPPLEMENTARY NOTES The views and conclusions contained herein are those of the authors and should not be interpreted as necessarily representing the official policies or endorsements, either expressed or implied, of the Air Force Office of Scientific Research or the U.S. Government.					
12 a. DISTRIBUTION / AVAILABILITY STATEMENT Approved for Public Release					
12 b. DISTRIBUTION CODE A					
13. ABSTRACT (Maximum 200 words) This report summarizes the research carried out under Grant F49620-03-1-0201 on the development of least-squares based finite element models of viscous compressible and incompressible flows as well as shear deformable plates and shells. The main objective of this research was to develop a robust and accurate computational methodology based on least-squares variational principles for the numerical solution of the equations governing plates and shells and viscous incompressible and compressible fluid flows. The use of least-squares principles leads to a variationally unconstrained minimization problem, where compatibility conditions between approximation spaces -such as inf-sup conditions -- never arise. Furthermore, the resulting linear algebraic problem will always have a symmetric positive definite (SPD) coefficient matrix, allowing the use of robust and fast preconditioned conjugate gradient methods for its solution. In this research, the basic theory of least-squares finite element formulations of the equations governing viscous incompressible flows and shear deformable theories of plate and shell structures was carried out and their application through a variety of benchmark problems was illustrated. In the case of fluid flows, penalty least-squares finite element models using high p -levels and low penalty parameters were developed as a good alternative to mixed least-squares finite element models, also developed in the research.					
14. SUBJECT TERMS Least-squares finite element models, Navier-Stokes equations, plates and shells, numerical simulations, accuracy and robustness				15. NUMBER OF PAGES 33 including cover page	
				16. PRICE CODE	
17. SECURITY CLASSIFICATION OR REPORT UNCLASSIFIED	18. SECURITY CLASSIFICATION ON THIS PAGE UNCLASSIFIED	19. SECURITY CLASSIFICATION OF ABSTRACT UNCLASSIFIED	20. LIMITATION OF ABSTRACT UL		

NSN 7540-01-280-5500

Standard Form 298 (Rev.2-89)
Prescribed by ANSI Std. Z39-18
298-102

Approved for public release,
distribution unlimited

REPORT DOCUMENTATION PAGE (SF298)
(Continuation Sheet)

1. LIST OF MANUSCRIPTS

- V. Prabhakar and J. N. Reddy, "A Stress Based Least-Squares Finite Element Model for Incompressible Navier-Stokes Equations," *International Journal of Computational Methods for Fluids*, in review.
- V. Prabhakar and J. N. Reddy, "Orthogonality of Modal Bases," *International Journal of Computational Methods for Fluids*, accepted for publication.
- V. Prabhakar and J. N. Reddy, "Spectral/ hp penalty least-squares finite element formulation for the steady Navier-Stokes equations," *Journal of Computational Physics*, in press.
- J. P. Pontaza and J. N. Reddy, "Least-squares finite element formulations for viscous incompressible and compressible fluid flows," *Computer Methods in Applied Mechanics and Engineering*, in press.
- J. P. Pontaza and J. N. Reddy, "Least-squares finite element formulations for one-dimensional radiative transfer," *Journal of Quantitative Spectroscopy & Radiative Transfer*, **95**(3), 387-406, 2005.
- J. P. Pontaza and J. N. Reddy, "Least-squares finite element formulation for shear-deformable shells," Special Issue on Shells: *Computer Methods in Applied Mechanics and Engineering*, **194**(21-24), 2464-2493, 2005.
- J. P. Pontaza and J. N. Reddy, "Mixed plate bending elements based on least-squares formulation," *International Journal for Numerical Methods in Engineering*, **60**(5), 891-922, 2004.
- J. P. Pontaza and J. N. Reddy, "Space-time coupled spectral/ hp least-squares finite element formulation for the incompressible Navier-Stokes equations," *Journal of Computational Physics*, **197**(2), 418-459, 2004.
- J. P. Pontaza, Xu Diao, J. N. Reddy, and K. S. Surana, "Least-squares finite element models of two-dimensional compressible flows," *Finite Elements in Analysis and Design*, **40**(5-6), 629-644, 2004.
- J. P. Pontaza and J. N. Reddy, "Spectral/ hp least-squares finite element formulation for the Navier-Stokes equations," *Journal of Computational Physics*, **190**(2), 523-549, 2003.
- J. N. Reddy, *An Introduction to Nonlinear Finite Element Analysis*, Oxford University Press, Oxford, UK, 2004.

2. SCIENTIFIC PERSONNEL and HONORS AND AWARDS

Vivek Prabhakar	Ph. D. Student, Texas A&M University
Juan P. Pontaza	Research Associate (Ph.D. student and Post-doc), Texas A&M University
J. N. Reddy	Distinguished Professor, Texas A&M University

- J. N. Reddy, **Computational Solid Mechanics Award** of The US Association for Computational Mechanics, July 2003.
- Juan P. Pontaza, Recipient of the **Robert J. Melosh Medal** for best paper on finite element analysis (based on the least-squares finite element formulation), Sponsored by the International Association of Computational Mechanics (IACM), 2004.
- J. N. Reddy, **Fellow** of the American Institute of Aeronautics and Astronautics (AIAA), May 2005.
- J. N. Reddy, **Distinguished Scientist Award** of the Sigma Xi, Texas A&M University, March 2005.

- J. N. Reddy, **Distinguished Research Award** of the American Society of Composites, October 2004.

3. INVENTIONS None

4. SCIENTIFIC PROGRESS AND ACCOMPLISHMENTS

The following research has been accomplished:

- Developed mixed least-squares finite element models of the Navier Stokes equations governing viscous incompressible flows.
- Developed space-time coupled least-squares finite element models of non-stationary Navier Stokes equations governing viscous incompressible flows.
- Developed least-squares finite element models of equations governing viscous compressible flows.
- Developed least-squares finite element models of bending of shear deformable plates and shells.
- Developed penalty least-squares finite element models of the stationary Navier Stokes equations governing viscous incompressible flows.
- Developed weak k-version least-squares finite element models, allowing for h - and p -type nonconformities

5. TECHNOLOGY TRANSFER

The PI has made several presentations at AFRL during 2003 and 2004 calendar years. The AFRL points of contact during the contract period of 2003-2005 are

- Daniel Strong, Design and Analysis Methods Branch, Structures Division, Bldg 146 Room 220, 58474, Air Force Research Laboratories, Wright-Patterson Air Force Base.
- Jose Camberos, Computational Sciences Branch, Aeronautical Sciences Division, Bldg 146 Room 225, 44043, Air Force Research Laboratories, Wright-Patterson Air Force Base.
- Robert A. Canfield, Air Force Institute of Technology.

MEMORANDUM OF TRANSMITTAL

Department of the Air Force
Air Force Office of Scientific Research
Directorate of Mathematics & Space Sciences
Computational Mathematics Program
Attn: Dr. Fariba Fahroo
875 North Randolph Street, Suite 325, Room 3112
Arlington, VA 22203

February 28, 2006

- ☐ Reprint (Orig + 2 copies) ☐ Technical Report (Orig + 2 copies)
☐ Manuscript (1 copy) ☒ Final Progress Report (2 copies)
☐ Other (1 copy) Interim Progress Report

CONTRACT/GRANT NUMBER: AFOSR Grant No. F49620-03-1-0201

REPORT TITLE:

Development of K-Version of the Finite Element Method: A Robust Mathematical and Computational Procedure

is forwarded for your information.

Sincerely,

J. N. Reddy
Distinguished Professor
Dept. of Mech. Engng.
Texas A&M University
College Station, TX 77843-3123

**DEVELOPMENT OF K-VERSION OF THE FINITE ELEMENT METHOD:
A ROBUST MATHEMATICAL AND COMPUTATIONAL PROCEDURE**

AFOSR Grant No. F49620-03-1-0201

J. N. Reddy

Department of Mechanical Engineering
Texas A&M University
College Station, Texas 77843-3123

Final Technical Report
submitted to

Department of the Air Force

Air Force Office of Scientific Research
Directorate of Mathematics & Space Sciences
Computational Mathematics Program

Attn: Dr. Fariba Fahroo, Program Manager, AFSOR/NM
875 North Randolph Street
Suite 325, Room 3112
Arlington, VA 22203

February 2006

20060727322

Acknowledgment/Disclaimer

This work was sponsored (in part) by the Air Force Office of Scientific Research, USAF, under grant/contract number F49620-03-1-0201. The views and conclusions contained herein are those of the authors and should not be interpreted as necessarily representing the official policies or endorsements, either expressed or implied, of the Air Force Office of Scientific Research or the U.S. Government.

Personnel Supported on the Grant

1. J. N. Reddy
Distinguished Professor, Texas A&M University, College Station
2. Juan P. Pontaza
Research Associate (Post-doc), Texas A&M University, College Station
3. Vivek Prabhakar
Ph. D. Student, Texas A&M University, College Station

AFRL Points of Contact

- Daniel Strong, Design and Analysis Methods Branch, Structures Division, Bldg 146 Room 220, 58474, Air Force Research Laboratories, Wright-Patterson Air Force Base.
- Jose Camberos, Computational Sciences Branch, Aeronautical Sciences Division, Bldg 146 Room 225, 44043, Air Force Research Laboratories, Wright-Patterson Air Force Base.
- Robert A. Canfield, Air Force Institute of Technology.

The PI has made several presentations at AFRL during 2003 and 2004 calendar years.

Honors and Awards Received During the Grant

1. J. N. Reddy, **Computational Solid Mechanics Award** of the US Association for Computational Mechanics, July 2003.
2. Juan P. Pontaza, Recipient of the **Robert J. Melosh Medal** for best paper on finite element analysis (based on the least-squares finite element formulation), Sponsored by the International Association of Computational Mechanics (IACM), 2004.
3. J. N. Reddy, **Fellow** of the American Institute of Aeronautics and Astronautics (AIAA), May 2005.
4. J. N. Reddy, **Distinguished Scientist Award** of the Sigma Xi, Texas A&M University, March 2005.
5. J. N. Reddy, **Distinguished Research Award** of the American Society of Composites, October 2004.
6. J. N. Reddy, The Dow Chemical **Best Paper Award** for the paper "Assessment of Plastic Failure of Polymers due to Surface Scratches," (with G. T. Lim and H.-J. Sue) in the General Category of the Failure Analysis and Prevention Special Interest Group at ANATECH 2004, Chicago, 2004.
7. J. N. Reddy, "Computational Modelling of Advanced Materials and Structures," **Keynote Lecture** of the *VII National Congress on Applied and Computational Mechanics*, vora, Portugal, April 14-16, 2003.
8. J. N. Reddy, "Novel Computational Procedures for Modeling of Problems of Mechanics," **Seth Memorial Lecture**, *48th ISTAM (Indian Society of Theoretical and Applied Mechanics) Congress*, Dec. 18-21, 2003, Birla Institute of Technology (BIT) Mesra, Ranchi, INDIA.
9. J. N. Reddy, "A Robust Computational Methodology for Numerical Simulation of Physical Processes," **Guest and Plenary Lecture** (and Guest of Honor) at the *International Conference on Theoretical, Applied, Computational and Experimental Mechanics* (ICTACEM 2004), Indian Institute of Technology, Kharagpur, India, December 28-30, 2004.
10. J. N. Reddy, "Computational Modelling of Materials and Structures and New Computational Methodology," **Invited Lecture** at the *US-Africa Workshop on Mechanics and Materials*, University of Cape Town, South Africa, January 23-28, 2005.
11. J. N. Reddy, "Advances in Computational Modelling of Materials and Structures," **Key Note Lecture** at the *Fifth International Conference on Composite Science & Technology* (ICCT'05) and *International Conference on Modelling, Simulation & Applied Optimization* (ICMSAO'05), American University of Sharjah, Sharjah (UAE), February 1-3, 2005.

12. J. N. Reddy, "A Refined Finite Element for Geometrically Nonlinear Analysis of Shell Structures," **Key Note Lecture** at the *5th International Conference on Computation of Shell and Spatial Structures*, June 1-4, 2005 Salzburg, Austria.
13. J. N. Reddy, "Refined Computational Models of Functionally Graded and Smart Structures and Materials," **Key Note Lecture** at *II ECCOMAS Thematic Conference on Smart Structures and Materials*, Instituto Superior Tecnico, Lisbon, Portugal, 18-21 July 2005.
14. J. N. Reddy, "Novel Computational Methods and Materials Modeling," **Plenary Lecture**, *XXVI Iberian Latin American Congress on Computational Methods in Engineering (CILAMCE 2005)*, October 19-21, 2005, Guarapari, Esprito Santo, Brazil.
15. J. N. Reddy, "A Consistent Shell Element for Nonlinear Analysis of Composite and Functionally Graded Structures," **Opening Plenary Lecture** (and Guest of Honor) at *International Conference on Advances in Structural Dynamics and Its Applications (ICASDA-2005)*, 7-9 December 2005, Visakhapatnam, Andhra Pradesh, India.
16. J. N. Reddy, "Least-Squares Based Finite Element Models for Problems in Structural Mechanics and Flows of Viscous Fluids," **Key Note Lecture** at *III European Conference on Computational Solid and Structural Mechanics*, Laboratrio Nacional de Engenharia Civil, Lisbon, Portugal, 5-8 June, 2006.

Journal Publications Under the Grant*

1. V. Prabhakar, J. N. Reddy, "A Stress Based Least-Squares Finite Element Model for Incompressible Navier-Stokes Equations," *International Journal of Computational Methods for Fluids*, in review.
2. V. Prabhakar, J. N. Reddy, "Orthogonality of Modal Bases," *International Journal of Computational Methods for Fluids*, accepted for publication.
3. V. Prabhakar, J. N. Reddy, "Spectral/*hp* penalty least-squares finite element formulation for the steady Navier-Stokes equations," *Journal of Computational Physics*, in press.
4. J. P. Pontaza, J. N. Reddy, "Least-squares finite element formulations for viscous incompressible and compressible fluid flows," *Computer Methods in Applied Mechanics and Engineering*, in press.
5. J. P. Pontaza, J. N. Reddy, "Least-squares finite element formulations for one-dimensional radiative transfer," *Journal of Quantitative Spectroscopy & Radiative Transfer*, v. 95(3), p. 387-406, 2005.
6. J. P. Pontaza, J. N. Reddy, "Least-squares finite element formulation for shear-deformable shells," Special Issue on Shells: *Computer Methods in Applied Mechanics and Engineering*, v. 194(21-24), p. 2464-2493, 2005.
7. J. P. Pontaza, J. N. Reddy, "Mixed plate bending elements based on least-squares formulation," *International Journal for Numerical Methods in Engineering*, v. 60(5), p. 891-922, 2004.
8. J. P. Pontaza, J. N. Reddy, "Space-time coupled spectral/*hp* least-squares finite element formulation for the incompressible Navier-Stokes equations," *Journal of Computational Physics*, v. 197(2), p. 418-459, 2004.
9. J. P. Pontaza, Xu Diao, J. N. Reddy, K. S. Surana, "Least-squares finite element models of two-dimensional compressible flows," *Finite Elements in Analysis and Design*, v. 40(5-6), p. 629-644, 2004.
10. J. P. Pontaza, J. N. Reddy, "Spectral/*hp* least-squares finite element formulation for the Navier-Stokes equations," *Journal of Computational Physics*, v. 190(2), p. 523-549, 2003.
11. J. N. Reddy, *An Introduction to Nonlinear Finite Element Analysis*, Oxford University Press, Oxford, UK, 2004.

*In addition, Professor Reddy has coauthored numerous papers on the subject of the grant with Professor K. S. Surana of the University of Kansas.

TECHNICAL REPORT

Abstract

This report summarizes the research carried out under Grant F49620-03-1-0201 on the development of least-squares based finite element models of viscous compressible and incompressible flows as well as shear deformable plates and shells. The main objective of this research was to develop a robust and accurate computational methodology based on least-squares variational principles for the numerical solution of the equations governing plates and shells and viscous incompressible and compressible fluid flows. The use of least-squares principles leads to a variationally unconstrained minimization problem, where compatibility conditions between approximation spaces – such as inf-sup conditions – never arise. Furthermore, the resulting linear algebraic problem will always have a symmetric positive definite (SPD) coefficient matrix, allowing the use of robust and fast preconditioned conjugate gradient methods for its solution. In this research, the basic theory of least-squares finite element formulations of the equations governing viscous incompressible flows and shear deformable theories of plate and shell structures was carried out and their application through a variety of benchmark problems was illustrated. In the case of fluid flows, penalty least-squares finite element models using high p -levels and low penalty parameters were developed as a good alternative to mixed least-squares finite element models, also developed in the research.

The new computational methodology offers many theoretical and practical advantages over traditional finite element formulations. In the context of solid mechanics, least-squares formulations are found to be robust for the bending of thin and thick plates, effective for the analysis of shell structures in bending and membrane dominated states, and yield accurate predictions of generalized displacements and stress resultants. In the context of fluid flows, least-squares formulations (both mixed and penalty models) have been implemented for viscous incompressible fluid flows. Mixed least-squares models are also implemented for compressible flows. In the mixed and penalty finite element model of viscous incompressible flows, high-order expansions are used to construct the discrete model. The element-by-element method and a matrix-free version of the conjugate gradient method with a Jacobi preconditioner are used to solve the linear system of equations. Numerical simulations are carried out for a number of two-dimensional benchmark problems, e.g., flow over a backward facing step and steady flow past a circular cylinder. The effect of penalty parameter on accuracy and computational cost is investigated thoroughly for these problems. The least-squares models are well suited for large scale computations and robust for moderately high Reynolds number and high Mach number flow conditions as well as for thick and thin structures.

We find that the k -version of least-squares (with $k = 1$), achieves equally accurate results when compared with formulations with $k = 0$, at a lower degree-of-freedom count. However, the construction of the $k = 1$ basis in the general multi-dimensional setting by one-dimensional tensor products has undesirable properties. For example, for geometrically distorted elements the spectral convergence property is lost. We proposed in this research the weak-enforcement of $k = 1$ continuity through the least-squares functional. In other words, the jump of the primary variables and their derivatives across inter-element boundaries is minimized in a least-squares sense, through the least-squares functional. This allows the use of practical $k = 0$ basis at the element level, and we achieve $k = 1$ continuity globally. In addition, the formulation naturally allows for geometric and basis non-conformities across inter-element boundaries.

1 Introduction

In the past few years finite element models based on least-squares variational principles have drawn considerable attention (see, e.g., [1, 2]). In particular, given a partial differential equation (PDE) or a set of partial differential equations, the least-squares method allows us to define an unconstrained minimization principle so that a finite element model can be developed in a variational setting. The idea is to define the least-squares functional as the sum of the squares of the equations residuals measured in suitable norms of Hilbert spaces. Assuming the governing equations (augmented with suitable boundary conditions) have a unique solution, the least-squares functional will have a unique minimizer. Thus, by construction, the least-squares functional is always positive and convex, ensuring coerciveness, symmetry, and positive definiteness of the bilinear form in the corresponding variational problem. Moreover, if the induced energy norm is equivalent to a norm of a suitable Hilbert space, optimal properties of the resulting least-squares formulation can be established.

However, an optimal least-squares formulation may result in an impractical finite element model. The reconciliation that must exist between practicality and optimality in least-squares based finite element models is of great importance and was first recognized by Bochev and Gunzburger [3, 2]. The practicality of the resulting finite element model is, to a large extent, determined by the complexity of algorithm development and CPU solve time of the resulting discrete system of equations. Typically, the practicality is measured in terms of C^k continuity/regularity of the finite element spaces across inter-element boundaries. Ideally, a least-squares finite element model with " C^0 practicality" and full (mathematical) optimality is to be developed – unfortunately, this can seldom be achieved in a satisfactory manner.

Conforming discretizations require that the finite element space be spanned by functions that belong to the Hilbert space H^{2m} , in contrast to weak form Galerkin models which require only H^m regularity (due to the weakened differentiability requirements induced by the integration by parts). For the least-squares model, this

implies a minimum of C^1 regularity of the finite element spaces across inter-element boundaries for $m = 1$.

To reduce the higher regularity requirements, the PDE or PDEs are first transformed into an equivalent lower order system by introducing additional independent variables, sometimes termed auxiliary variables, and then formulating the least-squares model based on the equivalent lower order system. The additional variables imply an increase in cost, but can be argued to be beneficial as they may represent physically meaningful variables, e.g., fluxes or stresses, and will be directly approximated in the model. Such an approach, is believed to be first explored by Jespersen [4] and is the preferred approach in modern implementations of least-squares finite element models. For 2nd order PDEs, an equivalent first-order system is introduced, and if the least-squares functional is defined in terms of L_2 norms only, the finite element model allows the use of nodal/modal expansions with merely C^0 regularity.

We also investigate a least-squares formulation where the “ C^0 practicality” is relaxed and finite element spaces are allowed to retain higher regularity across inter-element boundaries. Such formulations do not require that auxiliary variables be introduced. We present a formulation where C^1 continuity is enforced in a weak sense through the least-squares functional thus still allowing the use of practical C^0 nodal/modal element expansions. The latter approach naturally allows for h - and p -type non-conformities in the computational domain and may be viewed as a discontinuous least-squares finite element formulation.

In this report we give a brief overview of the work. Specifically, in Section 2 we present least-squares formulations using a unified approach for an abstract initial boundary value problem, which could represent a mathematical model describing fluid flow or the deformation of a solid structure. In Section 3 we present applications to fluid mechanics, for viscous incompressible flows, and in Section 4 applications to solid mechanics, for shear-deformable shell structures. We refer the reader to the journal publications under the grant for additional details on applications to incompressible and compressible flows [5, 6, 7, 11, 12], plates and shells [8, 9], and radiative transfer [10].

2 An abstract least-squares formulation

In this section we present the steps involved in developing and arriving at a least-squares based finite element model. We wish to present the procedure in a general setting, and to this end present the procedure in the context of an abstract initial boundary value problem.

2.1 Notation

Let $\bar{\Omega}$ be the closure of an open bounded region Ω in \mathbb{R}^d , where $d = 2$ or 3 represents the number of space dimensions, and $\mathbf{x} = (x_1, \dots, x_d) = (x, y, z)$ be a point in $\bar{\Omega} =$

$\Omega \cup \partial\Omega$, where $\partial\Omega = \Gamma$ is the boundary of Ω .

For $s \geq 0$, we use the standard notation and definition for the Sobolev spaces $H^s(\Omega)$ and $H^s(\Gamma)$ with corresponding inner products denoted by $(\cdot, \cdot)_{s,\Omega}$ and $(\cdot, \cdot)_{s,\Gamma}$ and norms by $\|\cdot\|_{s,\Omega}$ and $\|\cdot\|_{s,\Gamma}$, respectively. Whenever there is no chance of ambiguity, the measures Ω and Γ will be omitted from inner product and norm designations. We denote the $L_2(\Omega)$ and $L_2(\Gamma)$ inner products by $(\cdot, \cdot)_\Omega$ and $(\cdot, \cdot)_\Gamma$, respectively. By $\mathbf{H}^s(\Omega)$ we denote the product space $[H^s(\Omega)]^d$.

2.2 The abstract problem

Consider the following abstract initial boundary value problem:

$$\mathcal{L}_t(\mathbf{u}) + \mathcal{L}_x(\mathbf{u}) = \mathbf{f} \quad \text{in } \Omega \times (0, \tau] \quad (1)$$

$$\mathcal{G}(\mathbf{u}) = \mathbf{h} \quad \text{on } \Gamma \times (0, \tau] \quad (2)$$

in which \mathcal{L}_t and \mathcal{L}_x are partial differential operators in time and space respectively, acting on the vector \mathbf{u} of unknowns. For example, a transient scalar Poisson equation would have $\mathcal{L}_t(u) = \partial u / \partial t$ and $\mathcal{L}_x(u) = -\nabla^2 u$.

The vector valued function \mathbf{f} is a known forcing function, \mathcal{G} is a trace operator acting on \mathbf{u} , and \mathbf{h} represents a known vector valued function on the boundary. We assume initial conditions are given such that the problem is well posed and a unique solution exists.

2.3 A first-order system least-squares (FOSLS) formulation

The L_2 least-squares functional associated with the abstract initial boundary value problem is constructed by summing up the squares of the equations residuals in the L_2 norm and is given by

$$\mathcal{J}(\mathbf{u}; \mathbf{f}, \mathbf{h}) = \frac{1}{2} \left(\|\mathcal{L}_t(\mathbf{u}) + \mathcal{L}_x(\mathbf{u}) - \mathbf{f}\|_{0,\Omega \times (0,\tau]}^2 + \|\mathcal{G}(\mathbf{u}) - \mathbf{h}\|_{0,\Gamma \times (0,\tau]}^2 \right). \quad (3)$$

It is easy to see that the minimizer of (3) solves (1)-(2) and viceversa.

Note that in defining the FOSLS functional we must make two restrictions: (1) the temporal and spatial partial differential operators and trace operator are at most of first-order and (2) the least-squares functional is defined exclusively in terms of L_2 norms. These restrictions are necessary in order to ensure a pre-determined level of practicality in the resulting least-squares based finite element model: specifically, the permission to use finite element spaces with merely C^0 regularity across inter-element boundaries.

If the partial differential equations (PDEs) under consideration are not of first-order, the “ C^0 practicality” of the least-squares based finite element model comes at

an extra cost, implied in restriction (1); which requires that the partial differential operators be of first-order. This can always be achieved by introducing auxiliary variables until a first-order system is attained. The added cost might be viewed as beneficial, in the sense that the auxiliary variables may have physical relevance to the problem under consideration, e.g., fluxes, vorticity, or stresses.

2.4 A discontinuous least-squares (DLS) formulation

In the discontinuous least-squares formulation the functional is defined at the element level, so that jumps across inter-element boundaries may be minimized in the least-squares sense and global weak C^k , $k \geq 0$ is achieved:

$$\begin{aligned} \mathcal{J}(\mathbf{u}; \mathbf{f}, \mathbf{h}) &= \sum_{e=1}^{N_{el}} \mathcal{J}^e(\mathbf{u}^e; \mathbf{f}, \mathbf{h}); \\ \mathcal{J}^e(\mathbf{u}^e; \mathbf{f}, \mathbf{h}) &= \frac{1}{2} \left(\|\mathcal{L}_t(\mathbf{u}^e) + \mathcal{L}_x(\mathbf{u}^e) - \mathbf{f}\|_{0, \Omega^e \times (0, \tau]}^2 \right. \\ &\quad \left. + \|\mathcal{G}(\mathbf{u}^e) - \mathbf{h}\|_{0, \Gamma^e \cap \Gamma \times (0, \tau]}^2 + \sum_a \|\mathbf{u}^e - \mathbf{u}^a\|_{k, \Gamma^e \times (0, \tau]}^2 \right) \quad (4) \end{aligned}$$

where the superscript a denotes abutting elements to element e .

Unlike the FOSLS formulation, the partial differential operators need not be reduced to first-order provided the index k in the last residual measure minimizing jumps across inter-element boundaries is at minimum $k = n - 1$, where n is the order of the partial differential operator. In addition, practical C^0 basis may be used in this formulation, although even simpler L_2 subspaces would suffice. For $n > 1$, higher condition numbers are associated with this formulation due to the higher differentiability requirements.

2.5 Time stepping

2.5.1 Space-time coupled approach

Note that prior to defining functionals (3) or (4) we did not replace the temporal operator with a discrete equivalent. This results in a fully space-time coupled formulation, implied in the definition of functionals (3) or (4) where the L_2 norm is defined in space-time, i.e. $\|\cdot\|_{0, \Omega \times (0, \tau]}$ denotes the L_2 norm of the enclosed quantity in space-time:

$$\|u\|_{0, \Omega \times (0, \tau]}^2 = \int_0^\tau \int_\Omega |u|^2 d\Omega dt.$$

This implies, for example, that a two-dimensional time-dependent problem will be treated as a three-dimensional problem in space-time domain. When dealing with the stationary form of the equations the integral over time domain is simply dropped.

In the space-time coupled approach, the effects of space and time are allowed to remained coupled. There is no approximation of the initial boundary value problem. Instead, a basis is introduced in time domain to represent the time evolution of the independent variables.

Invariably, we as analysts would like to simulate and study the time evolution of an initial boundary value problem for large values of time. Taking into consideration modelling issues, we realize that this would require a space-time mesh with a large number of elements in time domain. The size of the resulting set of assembled algebraic equations could be large and prohibitively expensive in terms of available computer memory and non-optimal in terms of CPU solve time. To alleviate the drawbacks, we adopt a time-stepping procedure in which the solution is obtained for space-time strips in a sequential manner. The initial conditions for the current space-time strip are obtained from the latest space plane from the previous space-time strip. Hence, for each space-time strip we solve a true initial boundary value problem, by minimizing the following (e.g. FOSLS) functional in space-time domain:

$$\mathcal{J}(\mathbf{u}; \mathbf{f}, \mathbf{h}) = \frac{1}{2} \left(\left\| \mathcal{L}_t(\mathbf{u}) + \mathcal{L}_x(\mathbf{u}) - \mathbf{f} \right\|_{0, \Omega \times [t_s, t_{s+1}]}^2 + \left\| \mathcal{G}(\mathbf{u}) - \mathbf{h} \right\|_{0, \Gamma \times [t_s, t_{s+1}]}^2 \right) \quad (5)$$

where the interval $[t_s, t_{s+1}]$ can be taken arbitrarily large, i.e., there are no restrictions on the size of the interval. Additional details on this time stepping approach may be found in Pontaza and Reddy [6].

2.5.2 Space-time decoupled approach

Alternatively, the temporal operator can be represented by truncated Taylor series expansions in time domain, e.g. a backward Euler or trapezoidal rule approximation. First, the temporal operator in Eq. (1) is replaced by the discrete approximation:

$$\mathcal{L}_t(\mathbf{u}) \approx \mathcal{L}_{\Delta t}(\mathbf{u}^{s+1}, \mathbf{u}^{s-q}), \quad q = 0, 1, 2, \dots$$

where the time increment dependence of the discrete operator is explicit as well as its dependence on histories of previous time steps. For example, for $\mathcal{L}_t(u) = \partial u / \partial t$ a (backward Euler) first-order approximation would be $\mathcal{L}_{\Delta t}(u) = (u^{s+1} - u^s) / \Delta t$.

To march the problem in time, we must minimize the following (e.g. FOSLS) functional at each time step:

$$\mathcal{J}_{\Delta t}(\mathbf{u}; \mathbf{f}, \mathbf{h}) = \frac{1}{2} \left(\left\| \mathcal{L}_{\Delta t}(\mathbf{u}^{s+1}, \mathbf{u}^{s-q}) + \mathcal{L}_x(\mathbf{u}^{s+1}) - \mathbf{f}^{s+1} \right\|_{0, \Omega}^2 + \left\| \mathcal{G}(\mathbf{u}^{s+1}) - \mathbf{h}^{s+1} \right\|_{0, \Gamma}^2 \right) \quad (6)$$

where the dependence on the time increment $\Delta t = t_{s+1} - t_s$ is evident. This time stepping approach obviously has associated with it a much lower computational cost when compared with the space-time coupled approach, as the dimensionality of the problem is not increased.

2.6 The variational problem

Having defined the least-squares functional, the abstract least-squares minimization principle can be stated as:

$$\text{find } \mathbf{u} \in X \text{ such that } \mathcal{J}(\mathbf{u}; \mathbf{f}, \mathbf{h}) \leq \mathcal{J}(\mathbf{v}; \mathbf{f}, \mathbf{h}) \forall \mathbf{v} \in X \quad (7)$$

where X is a suitable vector space, e.g. $X = \mathbf{H}^1(\bar{\Omega})$ for a FOSLS space-time decoupled formulation.

The Euler-Lagrange equation for this minimization problem is given by the following variational problem:

$$\text{find } \mathbf{u} \in X \text{ such that } \mathcal{B}(\mathbf{u}, \mathbf{v}) = \mathcal{F}(\mathbf{v}) \forall \mathbf{v} \in X \quad (8)$$

where \mathcal{B} is a symmetric form given by

$$\mathcal{B}(\mathbf{u}, \mathbf{v}) = (\mathcal{L}(\mathbf{u}), \mathcal{L}(\mathbf{v}))_{\Omega} + (\mathcal{G}(\mathbf{u}), \mathcal{G}(\mathbf{v}))_{\Gamma}$$

and \mathcal{F} is a functional given by

$$\mathcal{F}(\mathbf{v}) = (\mathbf{f}, \mathcal{L}(\mathbf{v}))_{\Omega} + (\mathbf{h}, \mathcal{G}(\mathbf{v}))_{\Gamma}$$

where $\mathcal{L} = \mathcal{L}_{\Delta t} + \mathcal{L}_{\mathbf{x}}$.

The inclusion of the boundary residual in the least-squares functional allows the use of spaces X that are not constrained to satisfy the boundary condition (2). In such a case, the boundary condition (2) is enforced in a weak sense through the least-squares functional. This is a tremendous advantage of least-squares based formulations, as it allows boundary conditions that are computationally difficult to impose to be efficiently included in the least-squares functional. An example where this property becomes extremely useful is for viscous or inviscid compressible flow, where characteristic-based boundary conditions need to be prescribed at outflow/inflow boundaries. Of course, if the boundary condition (2) can be easily imposed and included in the space X , we omit the residual associated with the boundary term in the least-squares functional.

The abstract expressions given above for the symmetric form \mathcal{B} and functional \mathcal{F} are only valid when the partial differential operators are linear. For the case when the partial differential operators are nonlinear, the following more general expressions apply

$$\mathcal{B}(\mathbf{u}, \mathbf{v}) = (\mathcal{L}(\mathbf{u}), \delta \mathcal{L}(\mathbf{u}))_{\Omega} + (\mathcal{G}(\mathbf{u}), \delta \mathcal{G}(\mathbf{u}))_{\Gamma}$$

and

$$\mathcal{F}(\mathbf{v}) = (\mathbf{f}, \delta \mathcal{L}(\mathbf{u}))_{\Omega} + (\mathbf{h}, \delta \mathcal{G}(\mathbf{u}))_{\Gamma}$$

where it is understood that $\delta \mathbf{u} = \mathbf{v}$. In general, when the partial differential operators are nonlinear, the resulting form will be non-symmetric. Symmetry of the form is restored only when the Euler-Lagrange equation is linearized by Newton's method.

2.7 The finite element model

The finite element model is obtained by either restricting (8) to the finite dimensional subspace X_{hp} of the infinite dimensional space X , or equivalently by minimizing (3) with respect to the chosen approximating spaces. This process leads to the discrete variational problem given by

$$\text{find } \mathbf{u}^{hp} \in X_{hp} \text{ such that } \mathcal{B}(\mathbf{u}^{hp}, \mathbf{v}^{hp}) = \mathcal{F}(\mathbf{v}^{hp}) \quad \forall \mathbf{v}^{hp} \in X_{hp} \quad (9)$$

We proceed to define a discrete problem by choosing appropriate finite element subspaces for each of the components of the vector valued function \mathbf{u} . There are no restrictive compatibility conditions on the discrete spaces, so we choose the same finite element subspace for each of the primary variables.

2.8 Nodal/modal expansions

We present in this section some details on the high-order nodal/modal expansions used in this work. Advantages of using high-order methods include [13, 5, 6]: exponentially fast decay of error measures for smooth solutions, small diffusion and dispersion errors, better data volume over surface ratio allowing for high efficiencies in parallel processing, and higher efficiency/accuracy in long time integration of unsteady problems.

In a modal expansion, the finite element spaces are spanned by tensor products of the one-dimensional C^0 p -type hierarchical basis

$$\psi_i(\xi) = \begin{cases} \frac{1-\xi}{2} & i = 1 \\ \left(\frac{1-\xi}{2}\right) \left(\frac{1+\xi}{2}\right) P_{i-2}^{\alpha,\beta} & 2 \leq i \leq p, \quad p \geq 2 \\ \frac{1+\xi}{2} & i = p+1 \end{cases} \quad (10)$$

In definition (10), $P_p^{\alpha,\beta}$ are the Jacobi polynomials of order p . We use ultraspheric polynomials corresponding to the choice $\alpha = \beta$ with $\alpha = \beta = 0$ or 1.

Figure 1 shows the one-dimensional modal basis for the case $p = 5$. The linear basis or “hat-functions” ensure the C^0 continuity requirement across element boundaries and the p -bubbles hierarchically enrich the finite element space. Note that by construction the p -bubbles vanish at $\xi = -1$, $\xi = +1$ and have no nodes associated with them.

In a nodal expansion, the finite element spaces are spanned by tensor products of the one-dimensional C^0 spectral nodal basis

$$h_i(\xi) = \frac{(\xi - 1)(\xi + 1)L'_p(\xi)}{p(p+1)L_p(\xi_i)(\xi - \xi_i)} \quad (11)$$

In Eq. (11), $L_p = P_p^{0,0}$ is the Legendre polynomial of order p and ξ_i denotes the location of the roots of $(\xi - 1)(\xi + 1)L'_p(\xi) = 0$ in the interval $[-1, 1]$. The set of

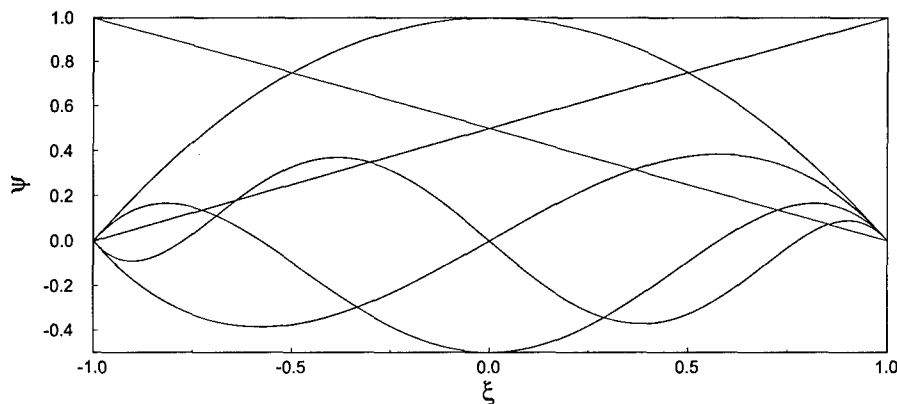


Figure 1: C^0 p -type hierarchical modal basis. Shown is the case of $p = 5$. The p -bubbles are scaled by a factor of 4, for viewing ease.

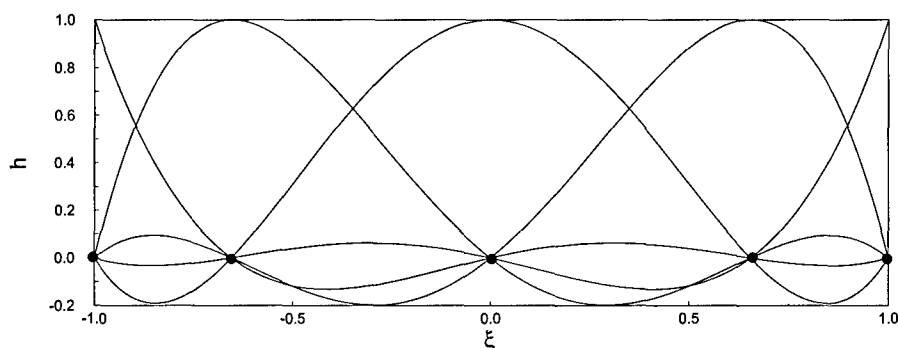


Figure 2: C^0 p -type (spectral) nodal basis. Shown is the case of $p = 4$.

points $\{\xi_i\}_{i=1}^{p+1}$ are commonly referred to as the Gauss-Lobatto-Legendre (GLL) points.

Figure 2 shows the one-dimensional nodal basis for the case $p = 4$. The location of the nodes coincides with the roots of the aforementioned Legendre polynomial and thus receives the name of a “spectral” basis. The Kronecker delta property is evident from the figure and is an attractive feature of this basis, as the coefficients coincide with nodal values.

3 Viscous incompressible fluid flows

The numerical solution of the incompressible Navier-Stokes equations using least-squares based finite element models is among the most popular applications of least-squares methods. Least-squares formulations for incompressible flow circumvent the

inf-sup condition, thus allowing equal-order interpolation of velocities and pressure, and result (after suitable linearization) in linear algebraic systems with a SPD coefficient matrix. This translates into easy algorithm development and leads to the use of robust and fast iterative solvers, resulting in substantial improvements over the traditional weak form Galerkin finite element model – where the finite element spaces for velocities and pressure must satisfy an inf-sup compatibility condition and one must deal with an un-symmetric and indefinite coefficient matrix.

3.1 The incompressible Navier-Stokes equations

We consider the solution of the Navier-Stokes equations governing incompressible flow, which in dimensionless form can be stated as follows:

Find the velocity $\mathbf{u}(\mathbf{x}, t)$ and pressure $p(\mathbf{x}, t)$ such that

$$\frac{\partial \mathbf{u}}{\partial t} + (\mathbf{u} \cdot \nabla) \mathbf{u} + \nabla p - \frac{1}{\text{Re}} \nabla^2 \mathbf{u} = \mathbf{f} \quad \text{in } \Omega \times (0, \tau] \quad (12)$$

$$\nabla \cdot \mathbf{u} = 0 \quad \text{in } \Omega \times (0, \tau] \quad (13)$$

$$\mathbf{u}(\mathbf{x}, 0) = {}^0\mathbf{u}(\mathbf{x}) \quad \text{in } \Omega \quad (14)$$

$$\mathbf{u} = \mathbf{u}^s \quad \text{on } \Gamma_u \times (0, \tau] \quad (15)$$

$$\hat{\mathbf{n}} \cdot \boldsymbol{\sigma} = \mathbf{f}^s \quad \text{on } \Gamma_f \times (0, \tau] \quad (16)$$

where $\Gamma = \Gamma_u \cup \Gamma_f$ and $\Gamma_u \cap \Gamma_f = \emptyset$. Re is the Reynolds number, $\nabla \cdot {}^0\mathbf{u} = 0$, \mathbf{f} is a dimensionless force, $\hat{\mathbf{n}}$ is the outward unit normal on the boundary of Ω , \mathbf{u}^s is the prescribed velocity on the boundary Γ_u , \mathbf{f}^s are the prescribed tractions on the boundary Γ_f , and in Eq. (14) the initial conditions are given. The conditions on the boundary Γ_f in Eq. (16) are used to model outflow conditions, with $\boldsymbol{\sigma} = -p\mathbf{I} + (1/\text{Re})\nabla\mathbf{u}$ and $\mathbf{f}^s = \mathbf{0}$.

As discussed in the previous section, in a FOSLS formulation the governing equations must be recast as an equivalent first-order system. This will allow the use of practical C^0 basis in the finite element model. We use a vorticity-based first-order system, using $\boldsymbol{\omega} = \nabla \times \mathbf{u}$, and in view of the vector identity

$$\nabla \times \nabla \times \mathbf{u} = -\nabla^2 \mathbf{u} + \nabla(\nabla \cdot \mathbf{u})$$

and the incompressibility constraint given in Eq. (13), the non-stationary Navier-Stokes equations, Eqs. (12)-(16), can be replaced by their first-order system equivalent:

Find the velocity $\mathbf{u}(\mathbf{x}, t)$, pressure $p(\mathbf{x}, t)$, and vorticity $\boldsymbol{\omega}(\mathbf{x}, t)$ such that

$$\frac{\partial \mathbf{u}}{\partial t} + (\mathbf{u} \cdot \nabla) \mathbf{u} + \nabla p + \frac{1}{\text{Re}} \nabla \times \boldsymbol{\omega} = \mathbf{f} \quad \text{in } \Omega \times (0, \tau] \quad (17)$$

$$\boldsymbol{\omega} - \nabla \times \mathbf{u} = \mathbf{0} \quad \text{in } \Omega \times (0, \tau] \quad (18)$$

$$\nabla \cdot \mathbf{u} = 0 \quad \text{in } \Omega \times (0, \tau] \quad (19)$$

$$\nabla \cdot \boldsymbol{\omega} = 0 \quad \text{in } \Omega \times (0, \tau] \quad (20)$$

$$\mathbf{u}(\mathbf{x}, 0) = {}^0\mathbf{u}(\mathbf{x}) \quad \text{in } \Omega \quad (21)$$

$$\mathbf{u} = \mathbf{u}^s \quad \text{on } \Gamma_u \times (0, \tau] \quad (22)$$

$$\boldsymbol{\omega} = \boldsymbol{\omega}^s \quad \text{on } \Gamma_\omega \times (0, \tau] \quad (23)$$

$$\hat{\mathbf{n}} \cdot \boldsymbol{\sigma} = \mathbf{f}^s \quad \text{on } \Gamma_f \times (0, \tau] \quad (24)$$

where $\Gamma_u \cap \Gamma_\omega = \emptyset$, i.e. if velocity is specified at a boundary, vorticity need not be specified there. This implies that no artificial boundary conditions for vorticity need to be devised at boundaries where the velocity is specified.

Other first-order systems are also possible, e.g. a stress-based first-order system or a velocity gradient based first-order system. Recasting the governing equations as a first-order system is not necessary when using the DLS formulation.

3.2 Numerical examples

3.2.1 Kovasznay flow

The first benchmark problem to be used for the purposes of verification is an analytic solution to the two-dimensional, stationary incompressible Navier-Stokes due to Kovasznay [14]. The spatial domain in which Kovasznay's solution is defined is taken here as the bi-unit square $\bar{\Omega} = [-0.5, 1.5] \times [-0.5, 1.5]$. The solution is given by

$$\begin{aligned} u(x, y) &= 1 - e^{\lambda x} \cos(2\pi y) \\ v(x, y) &= \frac{\lambda}{2\pi} e^{\lambda x} \sin(2\pi y) \\ p(x, y) &= p_0 - \frac{1}{2} e^{2\lambda x} \end{aligned} \quad (25)$$

where $\lambda = \text{Re}/2 - (\text{Re}^2/4 + 4\pi^2)^{1/2}$, p_0 is a reference pressure (an arbitrary constant), and we choose $\text{Re} = 40$.

Figure 3 shows p -convergence curves of the velocity field in the H^1 norm as a function of total number of degrees of freedom for the different formulations.

We see that spectral convergence of the velocity field is realized for all the formulations. However, the FOSLS formulations have a higher degree of freedom count due to the auxiliary variables used to recast the governing equations as an equivalent first-order system. From the numerical results it might appear that the DLS formulation is the formulation of choice. However, due to the higher order operators involved in the DLS formulation (e.g. the ∇^2 operator), the conditioning of the resulting coefficient matrix is higher.

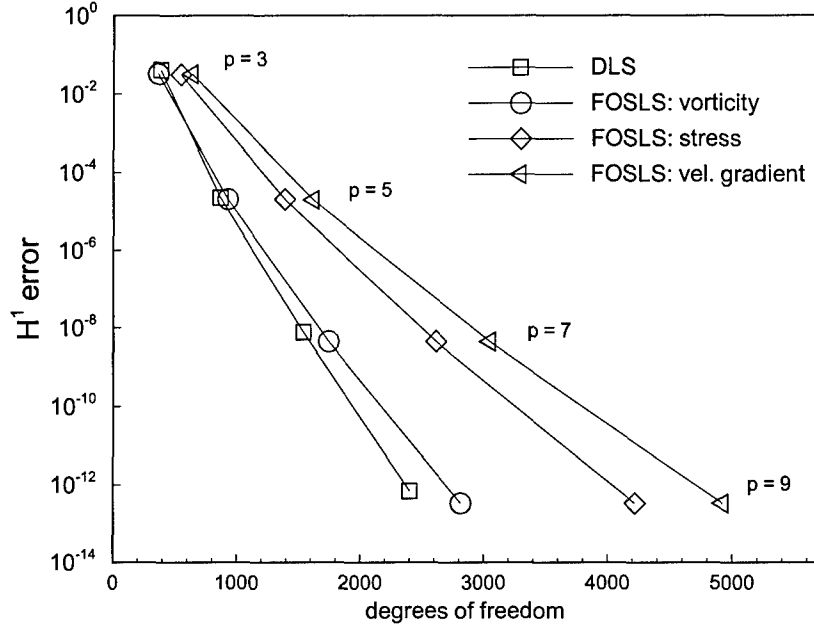


Figure 3: Convergence of the velocity field to the Kovasznay solution in the H^1 norm for FOSLS and DLS formulations.

3.2.2 Flow past two circular cylinders in a side-by-side arrangement

We consider two-dimensional flow of an incompressible fluid past two circular cylinders in a side-by-side arrangement. Both cylinders are equal in size, with diameter D , and face the free-stream. The flow around such an arrangement is characterized by three distinct flow regimes, depending on the gap size S between cylinder surfaces [15, 16].

The cylinders are of unit diameter and are at a distance $S/D = 0.85$ of each other. The simulation is carried out using a space-time coupled formulation. The connected model in space-time, $\bar{\Omega}^h \times [t_s, t_{s+1}]$, consists of 762 finite elements in space and a single element layer in time. Figure 4 shows the connected model in space and a close-up view of the geometric discretization around the circular cylinders.

We use nodal expansions with $p_\xi = p_\eta = 4$ and $p_\gamma = 2$ in each element, i.e. fourth-order expansions in space and a second-order expansion in time, resulting in $N_{\text{dof}} = 149,508$ for a space-time strip. At each Newton step the linear system of algebraic equations is solved using the matrix-free conjugate gradient algorithm with a Jacobi preconditioner. For the time marching procedure the size of the time step, $\Delta t = t_{s+1} - t_s$, was chosen as $\Delta t = 0.20$. We consider a Reynolds number of 100, based on the free-stream velocity and cylinder diameter.

At the upstream boundary of the computational domain both velocity components are assigned free-stream values: $u = u_\infty = 1$ and $v = 0$. At the lateral boundaries

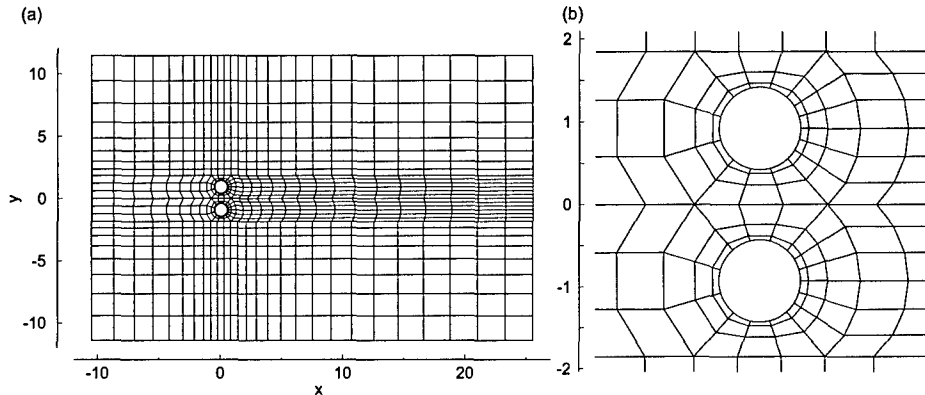


Figure 4: Computational domain and mesh for flow past two circular cylinders in a side-by-side arrangement, $S/D = 0.85$. (a) Connected model, $\bar{\Omega}^h$. (b) Close-up view of the geometric discretization around the circular cylinders.

a no-flux boundary condition is imposed: $\partial u / \partial y = 0$ and $v = 0$. No-slip boundary conditions are specified at the cylinder surface: $u = v = 0$. The outflow boundary condition is imposed in a weak sense through the least-squares functional.

At this gap size, we did not see (or expected) a well-defined periodic steady state. The simulation was thus carried out for $t \in [0, 400]$, by which time the flow exhibited “well-developed” characteristics such as intermittent bistable gap jets and amalgamation of gap vortices leading to the formation of a single large-scale vortex street.

Figure 5 shows instantaneous vorticity contours at (a) $t = 314$ and (b) $t = 352$, at which times the gap jet is “shooting” upwards and downwards respectively. In accordance with the experimental visualizations of Williamson [15], a single large-scale vortex street is formed downstream of the cylinders, by virtue of vortex interactions in the near-wake of the cylinders. Gap vortices from both cylinders are squeezed and amalgamated with dominant outer vortices, predominantly towards the narrow-wake side (the gap jet “shooting” direction).

In Fig. 6 we plot the force coefficient associated with the repulsive force experienced by the circular cylinder whose center is located at $(x, y) = (0, -0.925)$. At early times, $0 \leq t \leq 125$, we see a well-defined shedding frequency, due to shedding synchronization in antiphase. For $t > 150$, the flow becomes asymmetric due to the bistable biased gap flow.

The value of the L_2 least-squares functional for remained below 10^{-3} throughout the time marching procedure, meaning that conservation of mass and momentum are being satisfied to within 10^{-3} at all times – implying a time-accurate numerical simulation.

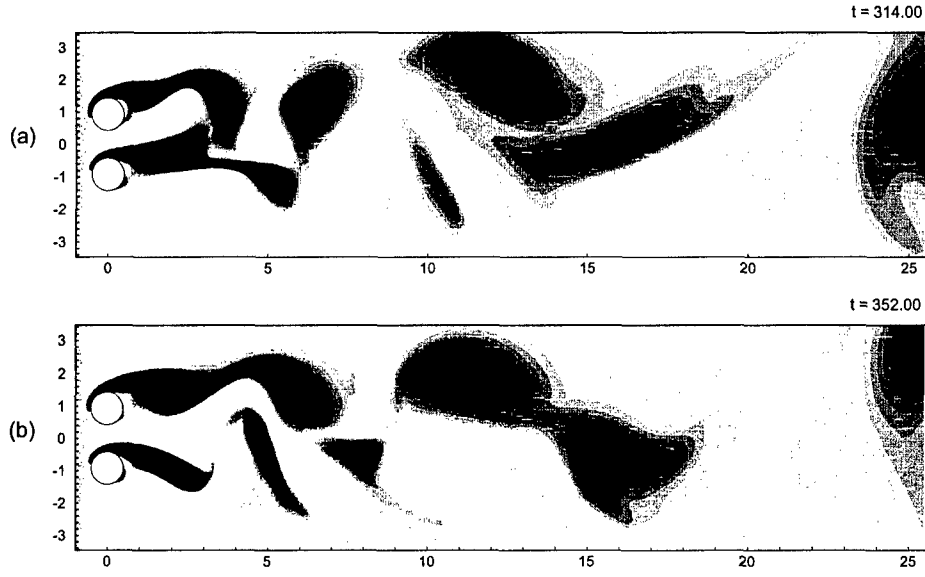


Figure 5: Instantaneous vorticity contours for the flow around two circular cylinders in a side-by-side arrangement with a gap size of $S/D = 0.85$ and $Re_D = 100$.

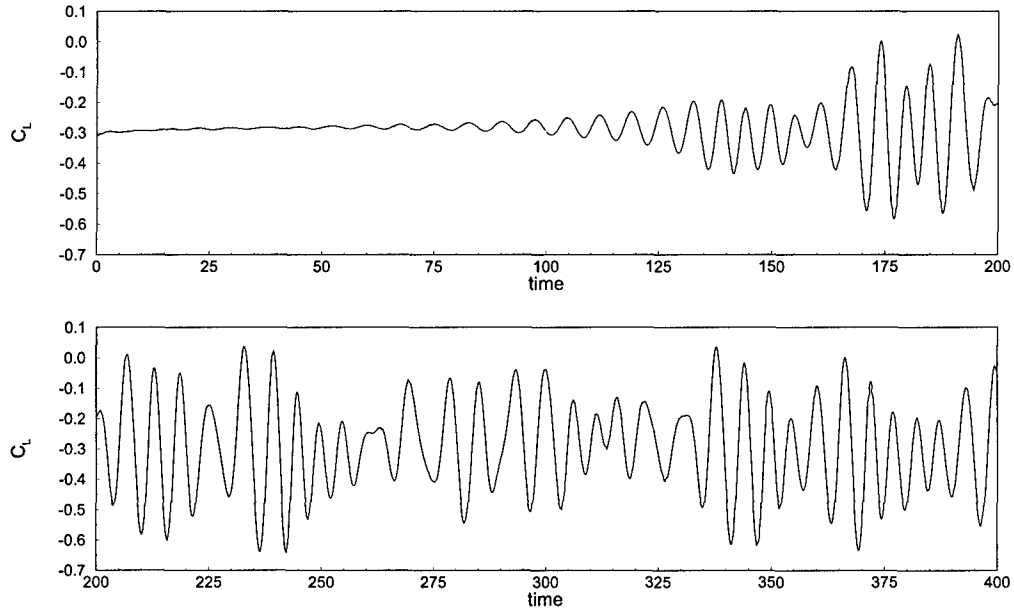


Figure 6: Time history of repulsive (lift) coefficient experienced by the circular cylinder whose center is located at $(x, y) = (0, -0.925)$.

4 Shear-deformable shells

Finite element formulations for the analysis of plates and shell structures are traditionally derived from the principle of virtual displacements or the principle of minimum total potential energy [17, 18]. When considering the limiting behavior of a shell as the thickness becomes small, for a given shell geometry and boundary conditions, the shell problem will in general fall into either a membrane dominated or bending dominated state – depending on whether the membrane or bending energy component dominates the total energy. Displacement-based finite element models have no major difficulties in predicting the asymptotic behavior of the shell structure in the membrane dominated case. However, computational difficulties arise in the case when the deformation is bending dominated. A strong stiffening of the element matrices occurs, resulting in spurious predictions for the membrane energy component. This phenomenon is known as *membrane-locking*. In shear-deformable shell models, yet another form of locking occurs and presents itself (again) in a strong stiffening of the element matrices, resulting in spurious predictions for the shear energy component. This form of locking is also present in plate bending analysis when the side-to-thickness ratio of the plate is large (i.e., when modelling thin plates). This locking phenomenon is known as *shear-locking*.

Least-squares finite element formulations for plates and shells have been shown to be robust with regards to membrane- and shear-locking and to yield highly accurate results for displacements as well as stresses (or stress resultants) [8, 9]. The formulations retain the generalized displacements and stress resultants as independent variables and, in view of the nature of the variational setting upon which the finite element model is built, allows for equal-order interpolation. In the following we present numerical results for a barrel vault (cylindrical shell) loaded by its own weight.

4.1 Governing equations

We consider circular cylindrical shells, where the shell mid-surface \mathcal{S} is given by

$$\mathcal{S} = \{-L < x_1 < L, x_2^2 + x_3^2 = R^2 \mid (x_1, x_2, x_3) \in \mathbb{R}^3\} \subset \mathbb{R}^3, \quad (26)$$

where $2L$ and R are the length and radius of the shell. The shell mid-surface \mathcal{S} , given by Eq. (26), can be parametrized by the single chart $\vec{\phi} = (\phi_1, \phi_2, \phi_3)$, $\vec{\phi} : \bar{\Omega} \subset \mathbb{R}^2 \longrightarrow \mathcal{S} \subset \mathbb{R}^3$,

$$\begin{aligned} \phi_1(\xi^1, \xi^2) &= \xi^1 \\ \phi_2(\xi^1, \xi^2) &= R \sin(\xi^2/R) \\ \phi_3(\xi^1, \xi^2) &= R \cos(\xi^2/R) \end{aligned} \quad (27)$$

so that Ω is the rectangle occupying the region

$$\{(\xi^1, \xi^2) \in \Omega \mid -L < \xi^1 < L, -R\pi < \xi^2 < R\pi\} \subset \mathbb{R}^2. \quad (28)$$

In Naghdi's shear-deformable shell model [19, 20], the membrane, bending, and shear strain measures $(\varepsilon_{\alpha\beta}, \chi_{\alpha\beta}, \zeta_\alpha)$ are [9]

$$\varepsilon_{11} = u_{1,1}, \quad 2\varepsilon_{12} = u_{1,2} + u_{2,1}, \quad \varepsilon_{22} = u_{2,2} + \frac{u_3}{R} \quad (29)$$

$$\chi_{11} = \theta_{1,1}, \quad 2\chi_{12} = \theta_{1,2} + \theta_{2,1} + \frac{u_{2,1}}{R}, \quad \chi_{22} = \theta_{2,2} + \frac{1}{R} \left(u_{2,2} + \frac{u_3}{R} \right) \quad (30)$$

$$\zeta_1 = u_{3,1} + \theta_1, \quad \zeta_2 = u_{3,2} + \theta_2 - \frac{u_2}{R} \quad (31)$$

and the equilibrium equations take the form

$$N_{,1}^{11} + N_{,2}^{12} + p^1 = 0 \quad (32)$$

$$N_{,1}^{12} + N_{,2}^{22} + \frac{M_{,1}^{12}}{R} + \frac{M_{,2}^{22}}{R} + \frac{Q^2}{R} + p^2 = 0 \quad (33)$$

$$Q_{,1}^1 + Q_{,2}^2 - \frac{N^{22}}{R} - \frac{M^{22}}{R^2} + p^3 = 0 \quad (34)$$

$$M_{,1}^{11} + M_{,2}^{12} - Q^1 = 0 \quad (35)$$

$$M_{,2}^{12} + M_{,2}^{22} - Q^2 = 0 \quad (36)$$

where u_α are the displacements of the shell mid-surface, u_3 is the out-of-plane displacement, θ_α are rotations of the transverse material fibers originally normal to the shell mid-surface, and $N^{\alpha\beta}$, $M^{\alpha\beta}$, Q^α are the membrane, bending, and shear thickness-averaged stress resultants. Here we employ the convention that Greek indices range over 1 and 2 and that “,” denotes differentiation.

The stress resultants are related to the strain measures through the following constitutive relations [19]

$$N^{11} = \frac{tE}{(1-\nu^2)} (\varepsilon_{11} + \nu \varepsilon_{22}), \quad N^{22} = \frac{tE}{(1-\nu^2)} (\nu \varepsilon_{11} + \varepsilon_{22})$$

$$N^{12} = \frac{tE}{(1+\nu)} \varepsilon_{12} \quad (37)$$

$$M^{11} = \frac{t^3 E}{12(1-\nu^2)} (\chi_{11} + \nu \chi_{22}), \quad M^{22} = \frac{t^3 E}{12(1-\nu^2)} (\nu \chi_{11} + \chi_{22})$$

$$M^{12} = \frac{t^3 E}{12(1+\nu)} \chi_{12} \quad (38)$$

$$Q^1 = \frac{tE}{2(1+\nu)} K_s \zeta_1, \quad Q^2 = \frac{tE}{2(1+\nu)} K_s \zeta_2 \quad (39)$$

where t is the thickness of the shell, E is the Young's modulus, ν is the Poisson's ratio, and K_s is the shear correction factor for the isotropic material. If we let $R \rightarrow \infty$

we recover the (linear) shear-deformable plate bending strain measures and governing equations, where membrane and bending effects are decoupled.

The equilibrium equations (32)-(36) and constitutive relations (37)-(39) are already of first-order and are used to define the least squares functional. The least-squares formulation and finite element model follow from the outline given in Section 2.

4.2 Numerical example: Barrel vault

We consider a barrel vault loaded by its own weight. The barrel vault is a segment of a circular cylindrical shell whose mid-surface, after being parametrized by (27), is given by

$$\Omega = \{(\xi^1, \xi^2) \mid -L < \xi^1 < L, -\frac{2\pi}{9}R < \xi^2 < \frac{2\pi}{9}R\}. \quad (40)$$

The barrel vault is simply-supported on rigid diaphragms on opposite edges and is free on the other two edges. For the described loading, geometry, and boundary conditions, the problem is popularly known as the Scordelis-Lo roof.

By symmetry considerations, the computational domain is limited to 1/4 of the total shell, so that

$$\Omega^h = \{(\xi^1, \xi^2) \mid 0 < \xi^1 < L, 0 < \xi^2 < \frac{2\pi}{9}R\}. \quad (41)$$

The geometry of the barrel vault is specified as follows: $2L = 50$ ft, $R = 25$ ft, and $t = 3$ in., so that $R/t = 100$. The material is homogeneous and isotropic with $E = 3 \times 10^6$ psi and $\nu = 0$. The shear correction factor K_s is specified as 5/6 and the self-weight loading as $p_z = 90$ lb/ft² uniformly distributed over the surface area of the vault.

The connected model, $\bar{\Omega}^h \subset \mathbb{R}^2$, consists of a 4×4 finite element mesh. For illustrative purposes we present in Fig. 7 the finite element mesh on the entire mid-surface of the barrel vault, $\mathcal{S} \subset \mathbb{R}^3$. The mesh is regular (i.e., not distorted) and graded. We expect strong boundary layers in the stress resultant profiles along the free and supported edges, so the mesh is graded towards those regions.

First, we present a convergence study in strain energy for increasing p -levels of the element approximation functions. An analytic value for the strain energy is not available, so we use instead a reference value. The reference value was obtained using displacement based weak form Galerkin elements with a p -level of 12. Denoting by \mathcal{U}^{ref} the reference strain energy of the barrel vault, the error measure is given by

$$E = \frac{|\mathcal{U}^{\text{ref}} - \mathcal{U}^{hp}|}{\mathcal{U}^{\text{ref}}}. \quad (42)$$

In Fig. 8 we plot the error measure E for the least-squares formulation as a function of the expansion order in a logarithmic-linear scale. We see from the convergence in

strain energy curve that an accurate least-squares solution is achieved for p -levels of 6 and higher.

Table 1 shows results for the vertical displacement and stress resultants at the center of the free edge of the barrel vault, $(\xi^1, \xi^2) = (0, \frac{2\pi}{9}R)$, for p -levels of 4, 6, 8, and 10. Similarly, in Table 2 we present results for the vertical displacement and stress resultants at the crown of the barrel vault, $(\xi^1, \xi^2) = (0, 0)$. We see from the tabulated data that the change in point values at p -levels of 6, 8, and 10 is negligible, and thus a converged numerical solution could be declared at p -levels of 6 or 8. The predicted vertical deflection at the center of the free edge (Table 1) is in good agreement with the shallow shell analytical value of 3.7032 in., the commonly used reference value for finite element analysis of 3.6288 in. [21], and the value of 3.6144 in. obtained using an assumed strain method in a fine mesh [22].

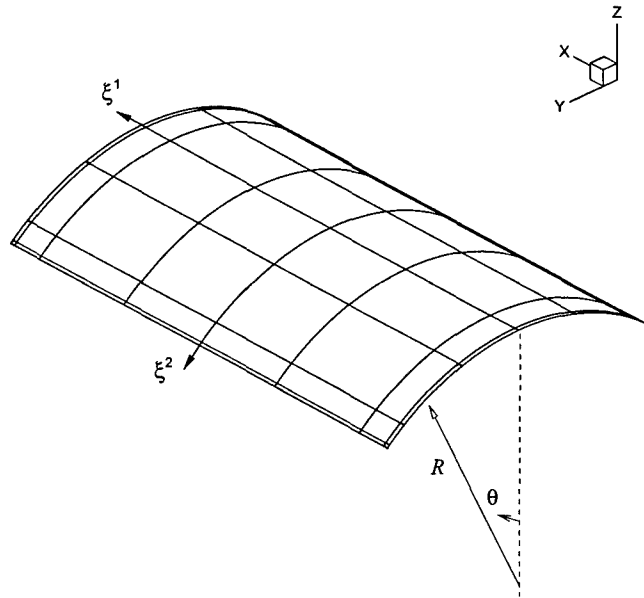


Figure 7: Finite element mesh on the entire mid-surface of the barrel vault, $\mathcal{S} \subset \mathbb{R}^3$, showing the surface coordinate system $(\xi^1, \xi^2) \in \mathbb{R}^2$.

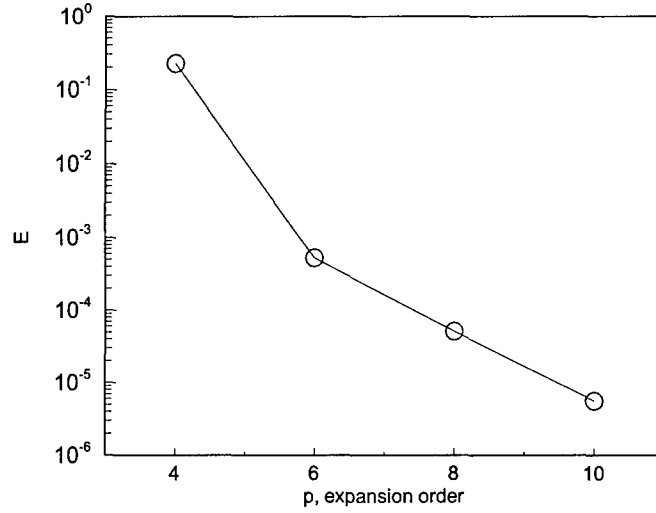


Figure 8: Convergence of strain energy for the barrel vault problem.

Table 1: p -convergence study showing vertical displacement and stress resultants at the center of the free edge of the barrel vault.

p level	w (in.)	N^{11} (kip/ft)	M^{11} (kip ft/ft)
4	-3.1208	68.3942	-0.5610
6	-3.6162	75.7476	-0.6400
8	-3.6173	75.7582	-0.6400
10	-3.6174	75.7593	-0.6400

Table 2: p -convergence study showing vertical displacement and stress resultants at the crown of the barrel vault.

p level	w (in.)	N^{11} (kip/ft)	N^{22} (kip/ft)	M^{11} (kip ft/ft)	M^{22} (kip ft/ft)
4	0.4109	-3.5870	-3.4148	0.0714	1.7597
6	0.5423	-1.5835	-3.4861	0.0959	2.0579
8	0.5425	-1.5805	-3.4862	0.0959	2.0583
10	0.5425	-1.5802	-3.4862	0.0959	2.0583

5 Scientific Progress and Accomplishments

A new computational methodology based on least-squares variational principles and the finite element method is developed for the numerical solution of the stationary and non-stationary Navier-Stokes equations governing viscous incompressible and compressible fluid flows and nonlinear equations governing shear deformation theories of plate and shell structures. The use of least-squares principles leads to a variationally unconstrained minimization problem, where compatibility conditions between approximation spaces - such as inf-sup conditions - never arise. Furthermore, the resulting linear algebraic problem will always have a symmetric positive definite (SPD) coefficient matrix, allowing the use of robust and fast preconditioned conjugate gradient methods for its solution. In the context of viscous incompressible flows, least-squares based formulations offer substantial improvements over the (traditional) weak form Galerkin finite element models - where the finite element spaces for velocities and pressure must satisfy an inf-sup compatibility condition and one must deal with an unsymmetric and indefinite coefficient matrix. In contrast, least-squares formulations circumvent the inf-sup condition, thus allowing equal-order interpolation of velocities and pressure, and result (after suitable linearization) in linear algebraic systems with a SPD coefficient matrix.

A penalty least-squares finite element model is also developed as a better alternative to traditional penalty finite element model. Advantage of the penalty least-squares finite element model is that it gives very accurate results for very low penalty parameters when used with high order element expansions. It is found that the computed pressure fields are continuous, and their values are found to be in excellent agreement with published results.

We have also developed a least-squares formulation, where regularity of order k is achieved by the weak enforcement of continuity constraints across inter-element boundaries. This allows for the use of practical $k = 0$ expansions at the element level, and can achieve any desired regularity at the global level. The formulation naturally allows for h - and p -type non-conformities.

The following research has been accomplished:

- Developed mixed least-squares finite element models of the Navier-Stokes equations governing viscous incompressible flows.
- Developed space-time coupled least-squares finite element models of non-stationary Navier-Stokes equations governing viscous incompressible flows.
- Developed least-squares finite element models of equations governing viscous compressible flows.
- Developed least-squares finite element models of bending of shear deformable plates and shells.

- Developed penalty least-squares finite element models of the stationary Navier-Stokes equations governing viscous incompressible flows.
- Developed weak k -version least-squares finite element models, allowing for h - and p -type nonconformity.

References

- [1] Jiang BN. *The Least-Squares Finite Element Method*. Springer-Verlag: New York, 1998.
- [2] Bochev PB, Gunzburger MD. Finite element methods of least-squares type. *SIAM Review* 1998; **40**:789–837.
- [3] Bochev PB. Analysis of least-squares finite element methods for the Navier-Stokes equations. *SIAM Journal of Numerical Analysis* 1997; **34**:1817–1844.
- [4] Jespersen D. A least-squares decomposition method for solving elliptic equations. *Mathematics of Computation* 1977; **31**:873–880.
- [5] Pontaza JP, Reddy JN. Spectral/ hp least-squares finite element formulation for the Navier-Stokes equations. *Journal of Computational Physics* 2003; **190**:523–549.
- [6] Pontaza JP, Reddy JN. Space-time coupled spectral/ hp least-squares finite element formulation for the incompressible Navier-Stokes equations. *Journal of Computational Physics* 2004; **197**:418–459.
- [7] Pontaza JP, Diao X, Reddy JN, Surana KS. Least-squares finite element models of two-dimensional compressible flows. *Finite Elements in Analysis and Design* 2004; **40**:629–644.
- [8] Pontaza JP, Reddy JN. Mixed plate bending elements based on least-squares formulation. *International Journal for Numerical Methods in Engineering* 2004; **60**:891–922.
- [9] Pontaza JP, Reddy JN. Least-squares finite element formulation for shear-deformable shells. *Computer Methods in Applied Mechanics and Engineering* 2005; **194**:2464–2493.
- [10] Pontaza JP, Reddy JN. Least-squares finite element formulations for one-dimensional radiative transfer. *Journal of Quantitative Spectroscopy & Radiative Transfer* 2005; **95**:387–406.
- [11] Pontaza JP, Reddy JN. Least-squares finite element formulations for viscous incompressible and compressible fluid flows. *Computer Methods in Applied Mechanics and Engineering*, in press.

- [12] Prabhakar V, Reddy JN. Spectral/*hp* penalty least-squares finite element formulation for the steady Navier-Stokes equations. *Journal of Computational Physics*, in press.
- [13] Karniadakis GE, Sherwin SJ. *Spectral/*hp* Element Methods for CFD*. Oxford University Press: Oxford, 1999.
- [14] Kovasznay LIG. Laminar flow behind a two-dimensional grid. *Proceedings of the Cambridge Philosophical Society* 1948; **44**:58–62.
- [15] Williamson CHK. Evolution of a single wake behind a pair of bluff bodies. *Journal of Fluid Mechanics* 1985; **159**:1–18.
- [16] Zdravkovich MM. *Flow Around Circular Cylinders, Vol. II*. Oxford University Press: Oxford, 2003.
- [17] Reddy JN. *Energy Principles and Variational Methods in Applied Mechanics* (2nd edn). John Wiley: New York, 2002.
- [18] Reddy JN. *An Introduction to Nonlinear Finite Element Analysis*. Oxford University Press: Oxford, UK, 2004.
- [19] Naghdi PM, Progress in Solid Mechanics, Vol. 4, Foundations of elastic shell theory, North-Holland, Amsterdam, 1963.
- [20] Reddy JN. *Mechanics of Laminated Plates and Shells. Theory and Analysis* (2nd edn). CRC Press: Boca Raton, FL, 2004.
- [21] MacNeal RH, Harder RL. A proposed standard set of problems to test finite element accuracy. *Finite Element Analysis and Design* 1985; **1**:3–20.
- [22] Chapelle D, Oliveira DL, Bucalem ML. MITC elements for a classical shell model. *Computers & Structures* 2003; **81**:523–533.